2020

Horizontal gene transfer of Fhb7 from fungus underlies Fusarium head blight resistance in wheat

Hongwei Wang
Shandong Agricultural University, wanghongwei@sdau.edu.cn

Silong Sun
Shandong Agricultural University

Wenyang Ge
Shandong Agricultural University

Lanfei Zhao
Shandong Agricultural University

Bingqian Hou
Shandong Agricultural University

See next page for additional authors

RESEARCH ARTICLE SUMMARY

PLANT SCIENCE

Horizontal gene transfer of *Fhb7* from fungus underlies *Fusarium* head blight resistance in wheat

Hongwei Wang*†, Silong Sun*, Wenyang Ge*, Lanfei Zhao*, Bingqian Hou*, Kai Wang*, Zhongfan Lyu*, Liyang Chen, Shoushen Xu, Jun Guo, Min Li, Peisen Su, Xuefeng Li, Guiping Wang, Cunyao Bo, Xiaojian Fang, Wenwen Zhuang, Xinxin Cheng, Jianwen Wu, Luhao Dong, Wuying Chen, Wen Li, Guilian Xiao, Jinxiao Zhao, Yongchao Hao, Ying Xu, Yu Gao, Wenjing Liu, Yanhe Liu, Huayan Yin, Jiazhu Li, Xiang Li, Yan Zhao, Xiaoqian Wang, Fei Ni, Xin Ma, Anfei Li, Steven S. Xu, Guihua Bai, Eviatar Nevo, Caixia Gao, Herbert Ohm, Lingrang Kong†

INTRODUCTION: *Fusarium* head blight (FHB) is a fungal disease that devastates global wheat production, with losses of billions of dollars annually. Unlike foliar diseases, FHB occurs directly on wheat spikes (inflorescences). The infection lowers grain yield and also causes the grain to be contaminated by mycotoxins produced by the *Fusarium* pathogen, thus imposing health threats to humans and livestock. Although plant breeders have improved wheat resistance to FHB, the lack of wheat strains with stable FHB resistance has limited progress.

RATIONALE: Many genetic loci in wheat affect FHB resistance but most only have minor effects; only a few exhibit a stable major effect on resistance. Wheat relatives in the Triticeae tribe carry resistant genes to different diseases including FHB and thus can be alternative sources of FHB resistance for wheat breeding. *Thinopyrum* wheatgrass has been used as a source of beneficial genes transferable to wheat by distant hybridization breeding since the 1930s. *Fhb7,* a gene transferred from *Thinopyrum* to wheat, showed a stable large effect on FHB resistance. However, the lack of a *Thinopyrum* reference genome hampered gene cloning and marker development, delaying the use of *Fhb7* in wheat breeding. Here, we cloned *Fhb7* using a reference assembly that we generated for *Th. elongatum* and characterized its resistance mechanisms and evolutionary history.

RESULTS: Using sequence data from *Th. elongatum*, we assembled the Triticeae E reference genome with 44,474 high-confidence genes annotated. Using this reference, we genetically mapped *Fhb7* and located it to a 245-kb genomic region. We determined a gene encoding a glutathione S-transferase (GST) as *Fhb7* by virus-induced gene silencing and evaluated mutants and transgenic plants. We discovered that Fhb7 detoxifies pathogen-produced trichothecene toxins by conjugating a glutathione (GSH) unit onto the epoxide moieties of type A and B trichothecenes. *Fhb7* GST homologs are absent in the plant kingdom, but one sequence showing ~97% identity with *Fhb7* was found in endophytic fungi of an *Epichloë* species that establishes symbiosis with temperate grasses. This result suggests that *Fhb7* might have been transferred from *Epichloë* to *Th. elongatum* through horizontal gene transfer. Finally, we demonstrated that *Fhb7*, when introgressed into diverse wheat backgrounds by distant hybridization, confers broad resistance to both FHB and crown rot without penalizing wheat yield. Our results suggest a source of *Fusarium* resistance for wheat improvement.

ON OUR WEBSITE

Read the full article at https://dx.doi.org/10.1126/science.aba5435

CONCLUSION: *Th. elongatum* carries biotic and abiotic resistance genes and is a useful resource for wheat breeding. The assembled *Th. elongatum* reference genome can aid identification and cloning of such genes for wheat improvement. Cloning of *Fhb7* revealed that it encodes a GST that can detoxify trichothecene toxins. Thus, *Fhb7* resistance differs from *Fhb1* resistance, which depends on a reduction of pathogen growth in spikes, although both confer durable resistance. The ability of *Fhb7* to detoxify multiple mycotoxins produced by various *Fusarium* species demonstrates its potential as a source of resistance to the various diseases for which *Fusarium* trichothecenes are virulence factors. The deployment of *Fhb7* in commercial wheat cultivars could alleviate both the food safety issue for consumers and the yield loss problem for growers. Sequence homologies between fungal and plant *Fhb7* suggested that horizontal gene transfer may help to shape plant genomes. ■

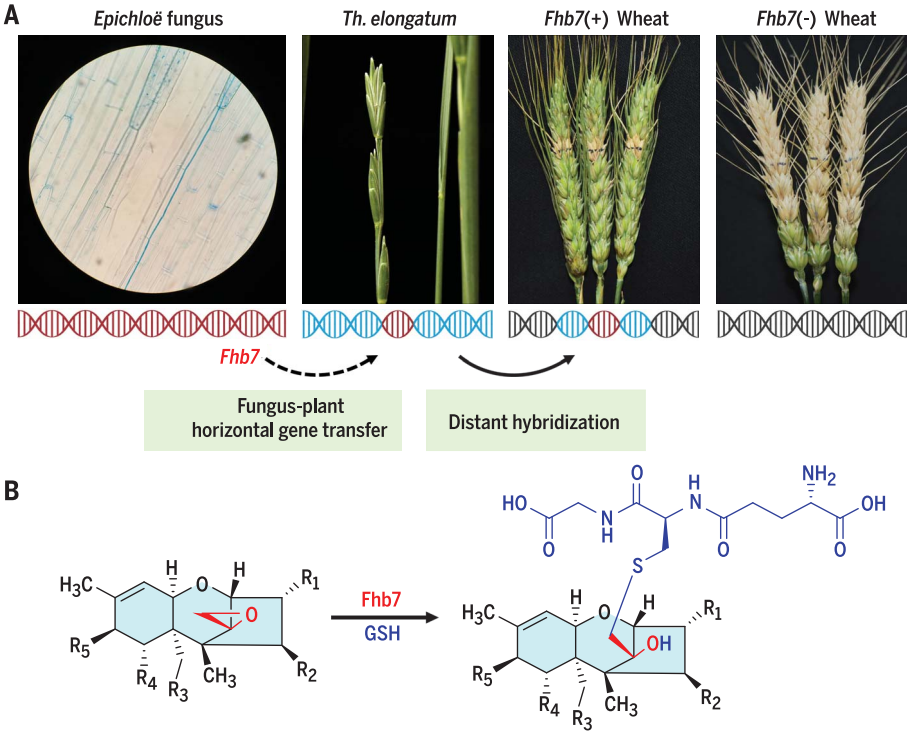

***Fhb7* confers FHB resistance by detoxifying trichothecenes.** (**A**) *Fhb7* in *Th. elongatum* genome likely came from an *Epichloë* fungus through horizontal gene transfer. *Fhb7* drives FHB resistance when introgressed from *Thinopyrum* into wheat. (**B**) *Fhb7* encodes a GST that detoxifies *Fusarium*-produced trichothecenes by conjugating GSH (blue) to the epoxy group (red). R_1 to R_5 refer to the variable groups in trichothecenes.

The list of author affiliations is available in the full article online.
*These authors contributed equally to this work.
†Corresponding author. Email: lkong@sdau.edu.cn (L.K.); wanghongwei@sdau.edu.cn (H.W.)
Cite this article as H. Wang *et al.*, *Science* **368**, eaba5435 (2020). DOI: 10.1126/science.aba5435

RESEARCH ARTICLE

PLANT SCIENCE

Horizontal gene transfer of *Fhb7* from fungus underlies *Fusarium* head blight resistance in wheat

Hongwei Wang[1]*†, Silong Sun[1]*, Wenyang Ge[1]*, Lanfei Zhao[1]*, Bingqian Hou[1]*, Kai Wang[2]*, Zhongfan Lyu[1]*, Liyang Chen[2], Shoushen Xu[1], Jun Guo[3], Min Li[1], Peisen Su[1], Xuefeng Li[1], Guiping Wang[1], Cunyao Bo[1], Xiaojian Fang[1], Wenwen Zhuang[1], Xinxin Cheng[1], Jianwen Wu[1], Luhao Dong[1], Wuying Chen[1], Wen Li[1], Guilian Xiao[1], Jinxiao Zhao[1], Yongchao Hao[1], Ying Xu[1], Yu Gao[1], Wenjing Liu[1], Yanhe Liu[1], Huayan Yin[1], Jiazhu Li[4], Xiang Li[1], Yan Zhao[1], Xiaoqian Wang[1], Fei Ni[1], Xin Ma[1], Anfei Li[1], Steven S. Xu[5], Guihua Bai[6], Eviatar Nevo[7], Caixia Gao[8], Herbert Ohm[9], Lingrang Kong[1]†

Fusarium head blight (FHB), a fungal disease caused by *Fusarium* species that produce food toxins, currently devastates wheat production worldwide, yet few resistance resources have been discovered in wheat germplasm. Here, we cloned the FHB resistance gene *Fhb7* by assembling the genome of *Thinopyrum elongatum*, a species used in wheat distant hybridization breeding. *Fhb7* encodes a glutathione S-transferase (GST) and confers broad resistance to *Fusarium* species by detoxifying trichothecenes through de-epoxidation. *Fhb7* GST homologs are absent in plants, and our evidence supports that *Th. elongatum* has gained *Fhb7* through horizontal gene transfer (HGT) from an endophytic *Epichloë* species. *Fhb7* introgressions in wheat confers resistance to both FHB and crown rot in diverse wheat backgrounds without yield penalty, providing a solution for *Fusarium* resistance breeding.

Wheat (*Triticum aestivum* L.) is a leading source of calories for the human population (*1*). The prevalence and widespread outbreaks of the devastating *Fusarium* head blight (FHB) disease, exacerbated by recent changes in climate and certain cropping practices, has posed a threat for global wheat production and food safety. *Fusarium* species cause not only FHB in wheat, barley, and oat, but also crown rot in wheat and ear rot in maize. However, *F. graminearum* is the prominent pathogen of wheat FHB in China, the United States, Canada, Europe, and many other countries (*2*). *Fusarium* produces epoxy-sesquiterpenoid compounds known as trichothecenes, some examples of which are deoxynivalenol (DON), T-2 toxin, HT-2 toxin, and nivalenol (NIV), among others; these compounds are inhibitors of protein synthesis and virulence factors for pathogenicity (*2*). Trichothecene contamination in cereal grain results in immunotoxicity and cytotoxicity in humans and animals and thus has aroused public safety concerns (*3*). Despite global screening efforts examining tens of thousands of wheat accessions, a limited number of quantitative trait loci (QTLs) have been verified to confer a stable effect on FHB resistance (*4*). *Fhb1* on chromosome 3B is the only QTL that has been used in breeding programs worldwide. Although it has been cloned from different Chinese wheat sources, its molecular identity and resistance mechanisms remain equivocal (*5*–*8*).

Wheat relatives have proven to be alternative sources for improvement of resistance to both biotic and abiotic stresses in wheat (*9*). Distant hybridization, the practice of making crosses between two different species, genera, or higher-ranking taxa, makes it possible to transfer alien genes from Triticeae tribe relatives to wheat (*9*–*11*). Tall and intermediate wheatgrasses of the *Thinopyrum* genus (forage grasses) are sources of resistance to salinity, drought, and disease for wheat. Several disease resistance genes, including stem rust (e.g., *Sr24*, *Sr25*, *Sr26*, *Sr43*, *Sr44*, and *SrB*), leaf rust (*Lr19*, *Lr24*, *Lr29*, and *Lr38*), powdery mildew (*Pm40* and *Pm43*), barley yellow dwarf virus (*Bdv2* and *Bdv3*), and *Fusarium* head blight (*Fhb7*), have been introduced from *Thinopyrum* into wheat for resistance breeding (*10*, *12*–*16*).

Fhb7 is a QTL introduced from *Thinopyrum elongatum* and shows a similar effect on FHB resistance as *Fhb1*. *Th. elongatum* (syn. *Agropyron elongatum* or *Lophopyrum elongatum*), a grass of the Triticeae family with a diploid E genome ($2n = 2x = 14$), is native to Eurasia and is thought to be a genome donor species for various tetra-, hexa-, and even decaploid species in the *Thinopyrum* genus (*14*). The lack of a reference sequence for the E genome has impeded the process of cloning and the development of diagnostic markers for the deployment of *Fhb7* and other E genome–derived resistance genes. Here, we report the assembly of a reference genome for *Th. elongatum* and describe the cloning and biomolecular characterization of *Fhb7*. Using the newly assembled E genome reference, we identified a GST gene as a candidate for *Fhb7* by map-based cloning and confirmed its function in FHB resistance using transgenics. Fhb7 can detoxify trichothecenes by catalyzing the conjugation of a glutathione (GSH) unit onto their toxic epoxide moiety. *Fhb7*'s coding sequence has no obvious homology to any known sequence in the entire plant kingdom but shares 97% sequence identity with a species of endophytic fungus (*Epichloë aotearoae*) known to infect temperate grasses, which provides evidence that *Fhb7* in the *Th. elongatum* genome might be derived from the fungus through HGT. We demonstrate here that *Fhb7* confers resistance to both FHB and crown rot without yield penalty in wheat.

Results

Th. elongatum genome assembly and evolution

To sequence and assemble the genome of *Th. elongatum*, 1.1 Tb of high-quality sequence reads were generated from a series of libraries, which is about 236× coverage of the *Th. elongatum* genome (table S1). We initially assembled the short sequence reads using DeNovoMAGICTM3.0 software (NRGene) and then filled the gaps using ~145 Gb (~31×) PacBio SMRT reads. The initial assembly was finely tuned using high-quality paired-end polymerase chain reaction (PCR)–free reads. Two Bionano optical maps (based on enzymes BspQI and DLE1 data) were further used to extend the scaffolds (tables S2 and S3), which resulted in a 4.63-Gb assembly with a contig N50 size of 2.15 Mb and a scaffold N50 size of 73.24 Mb (Table 1).

To construct the pseudochromosomes, high-throughput chromosome conformation capture (Hi-C) data were used to categorize and order the assembled scaffolds (table S4). A total of 141 scaffolds were anchored and oriented onto seven pseudochromosomes, which account for 95% of the estimated genome size (4.78 Gb; fig. S1) and 98% of the assembled genome sequences (fig. S2). About 97.6% complete and 1.3% fragmented Embryophyta genes were detected in our assembly according to BUSCO [Benchmarking Universal Single-Copy Orthologs (*17*)], proportions comparable

[1]State Key Laboratory of Crop Biology, College of Agronomy, Shandong Agricultural University, Tai'an, Shandong 271018, PR China. [2]Novogene Bioinformatics Institute, Beijing 100083, PR China. [3]Crop Research Institute, Shandong Academy of Agricultural Sciences, Jinan, Shandong 250100, PR China. [4]College of Chemistry and Chemical Engineering, Yantai University, Yantai, Shandong 264005, PR China. [5]USDA-ARS, Cereal Crops Research Unit, Edward T. Schafer Agricultural Research Center, Fargo, ND 58102, USA. [6]USDA-ARS, Hard Winter Wheat Genetics Research Unit, Manhattan, KS 66506, USA. [7]Institute of Evolution, University of Haifa, Mount Carmel, Haifa 3498838, Israel. [8]State Key Laboratory of Plant Cell and Chromosome Engineering, Institute of Genetics and Developmental Biology, Chinese Academy of Sciences, Beijing 100101, PR China. [9]Department of Agronomy, Purdue University, West Lafayette, IN 47907, USA.
*These authors contributed equally to this work.
†Corresponding author. Email: lkong@sdau.edu.cn (L.K.); wanghongwei@sdau.edu.cn (H.W.)

Table 1. Summary statistics for *Th. elongatum* genome assembly.

Assembly characteristics	Values
Estimated genome size	**4.78 Gb**
Total length of contigs	4.58 Gb
N50 length of contigs	2.15 Mb
Total number of contigs	12,262
Longest contigs	11.6 Mb
Total length of scaffolds	4.63 Gb
N50 length of scaffolds	73.24 Mb
Total number of scaffolds	783
Longest scaffolds	258.71 Mb
Total gap size	52.78 Mb
Total sequences anchored to the pseudochromosomes	4.54 Gb
Number of annotated high-confidence genes	44,474
Percentage of repeat sequences	81.29%
Complete BUSCOs	97.6%
Fragmented BUSCOs	1.3%
Missed BUSCOs	1.1%

to other *Triticum* genomes (table S5). The quality of the E genome assembly was validated by assessment of the long terminal repeat (LTR) completeness using LTR Assembly Index (LAI) software (*18*) (table S6), by genomic alignment with 61 randomly selected bacterial artificial chromosome (BAC) clones (fig. S3 and table S7), and by the consistency of our assembly with a high-density genetic map from a hexaploid *Thinopyrum* species (*19*) (fig. S4).

Repetitive elements are dispersed throughout the E genome, with ~81.29% of the *Th. elongatum* assembly being annotated as repetitive elements, including retrotransposons (62.39%), DNA transposons (17.83%), and unclassified elements (1.07%) (table S8 and table S9). Analysis of the Cereba and Quinta LTR retrotransposons supported that the centromere regions were appropriately assembled (fig. S5). The composition of different classes of repetitive DNA in the E genome was similar to those of the wheat A, B, or D subgenomes (fig. S6). No recent LTR burst was detected in the E or common wheat genomes (fig. S7), suggesting relatively stable genomes and helping to explain the success of distant hybridization breeding efforts using these materials. A total of 44,474 high-confidence protein-coding genes were predicted on the basis of a combination of methods [ab initio, protein homology based, and RNA-sequencing (RNA-seq) based], and 44,144 (99.3%) of the predicted genes were anchored onto the seven assembled pseudochromosomes (figs. S8 and S9 and tables S10 to S12).

Gene family analysis identified 32,048 orthologous genes between the E genome and the wheat A, B, or D genome or the barley genome (fig. S10). A synonymous substitution rate (K_s) value was calculated using a moving-average model with the ortholog dataset, which revealed similar K_s peak values between the E genome and the wheat subgenomes (E and A: 0.0645, E and B: 0.0645, E and D: 0.062), indicating a branching time for *Th. elongatum* and *Triticum* of ~4.77 to 4.96 million years ago when a nucleotide substitution rate of $6.5*10^{-9}$ was used (Fig. 1A) (*20*).

We also compared the E genome with other Triticeae genomes that have been used for distant hybridization based on a maximum likelihood tree built using single-copy genes from available Triticeae genome assemblies; the tree also incorporated transcript data for several diploid species, including the Triticeae R, Q, V, F, and Ns genomes (table S13). The three wheat subgenomes are more closely related to the E genome of *Th. elongatum* than they are to the R genome of rye, another species frequently used in wheat distant hybridization (Fig. 1A). A syntenic block analysis indicated genome-wide colinearity between the E genome and the A, B, or D genomes, which helps to explain the success of E-genome–based distant hybridization breeding in wheat (Fig. 1B and data S1). Substantial colinearity notwithstanding, we did identify 18 fragmental inversions between the E genome and the wheat subgenomes, with sizes ranging from 1.5 to 18 Mb, which is supported by both the Bionano maps and Hi-C data (fig. S11 and table S14).

Map-based cloning of the *Fusarium* resistance gene *Fhb7*

A total of 1897 resistance gene analogs (RGA) were annotated in the E genome (fig. S12 and table S15). An apparent RGA expansion, especially for CC-NBS-LRR (CNL), on the distal end of the long arm of chromosome 7E (7EL) is accompanied with the expansion of this genomic region (fig. S13 and table S16). Some of the alien resistance gene introgressions into wheat are located in this region, including *Lr19*, *Sr25*, *Bdv3*, and *Fhb7* (*10*, *13*, *14*).

Previously, we mapped the *Fhb7* to the distal end of the 7EL (based on recombination between 7E1 and 7E2 in a common wheat background) using a recombinant inbred line (RIL) population from a cross between an FHB-susceptible substitution line (7E1/7D) and an FHB-resistant substitution line (7E2/7D) (*13*, *21*). For further mapping of this gene, we developed a segregation population derived from BC_6F_1 with the same cross, in which FHB resistance was tracked as monogenic trait for validation of phenotypes. We also developed a population to promote 7E recombination by introducing the CS *ph1bph1b* locus (fig. S14). Because of the semidominant nature of *Fhb7*, the homozygous offspring of the recombinants were evaluated for FHB resistance. With analysis of 258 recombinants (between the *XBE45653* and *XsdauK67* markers) screened from 19,200 progeny of BC_6F_1 population, we confirmed that *Fhb7* is positioned between the *XSdauK79* and *XSdauK80* markers within an ~1.2-Mb region based on the E reference genome (Fig. 1C and fig. S15).

Analysis of the RNA-seq data of E reference genome from *Th. elongatum* spikes identified eight expressed genes in the *Fhb7* region (Fig. 1C and table S17). However, when conducting transcriptomics analysis of the parental lines of 7E1/7D (S) and 7E2/7D (R), we found that only two candidate genes (Tel7E01T1020600.1 and Tel7E01T1021800.1) were expressed in a manner specific to the 7E2 genome (the resistant parent) and E reference genome [which also confers FHB resistance (*12*, *22*)] (Fig. 1C and tables S18 and S19). BAC clones containing Tel7E01T1020600.1 were identified from the resistant donor line and new markers (*XsdauK86* and *XsdauK87*) derived from the BAC ends were developed to screen recombinants among 5760 progeny of the segregation population harboring the CS *ph1bph1b* locus (Fig. 1C, fig. S14, and table S20). Analysis of phenotypic data of the three key recombinants verified that *Fhb7* is located between the *XsdauK86* and *XsdauK88* markers, thereby delineating this locus to a 245-kb region containing a single expressed gene: Tel7E01T1020600.1 (Fig. 1C). This gene is present in the E reference genome and 7E2 genome but absent in the susceptible 7E1 genome based on analysis of genomics and transcriptomics data (table S19 and table S21).

Gene expression analysis using quantitative PCR indicated that Tel7E01T1020600.1 was constitutively expressed in all tissues examined, including root, leaf, shoot, and spike (fig. S16). Moreover, barley stripe mosaic virus (BSMV)–induced gene silencing of Tel7E01T1020600.1 in wheat leaves revealed that it conferred

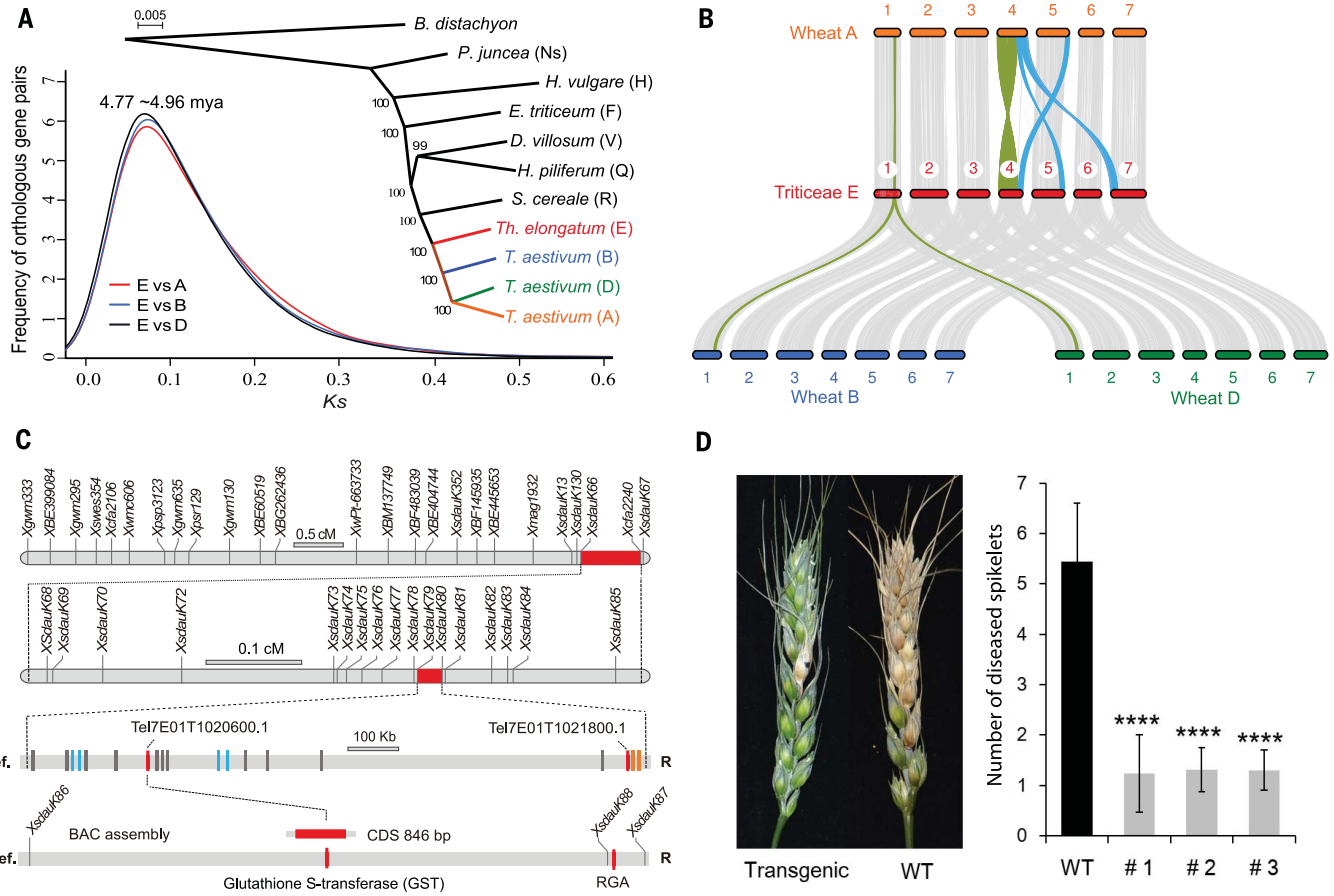

Fig. 1. Genome evolution of *Th. elongatum* and cloning of *Fhb7*. (**A**) Maximum likelihood phylogenetic tree of the genomes of Triticeae species and the Ks distributions of ortholog genes between the E genome and the wheat Chinese Spring A, B, and D subgenomes. mya, million years ago. (**B**) Syntenic blocks between the E genome and the three wheat subgenomes. The representative inversion fragment is indicated in green; chromosomal translocations for the wheat A subgenome compared with the E genome are also indicated in blue. (**C**) Map-based cloning of *Fhb7* at the distal region of chromosome 7E. Using the BC_6F_1 population derived from the cross between two wheat-*Thinopyrum* substitution lines, 7E1/7D and 7E2/7D, *Fhb7* was initially mapped to an interval between the markers *XsdauK79* and *XsdauK80* (~1.2 Mb on the E reference genome) (second bar from the top). The expressed genes are labeled as follows: gray refers to no expression in the E reference genome; blue refers to E reference genome–specific expression; orange refers to expression in the E reference, 7E1 and 7E2 genomes; red refers to expression in FHB-resistant donor genomes of 7E2 and E reference (third bar from the top). BAC clones containing Tel7E01T1020600.1 were identified from the substitution line 7E2/7D, based on which genetic markers (XsdauK86 and XsdauK87) were developed for recombinant screening of the CS *ph1bph1b* population. Finally, *Fhb7* was genetically confirmed within a 245-kb region between markers *XsdauK86* and *XsdauK88*, with only the candidate gene Tel7E01T1020600.1 encoding a GST [CDS is shown in red; untranslated region is shown in gray] (fourth bar from the top). (**D**) FHB was evaluated for wild-type (WT, KN199) and transgenic wheat KN199 expressing the native promoter and the 846-bp open reading frame of *Fhb7*. T_3 plants containing *Fhb7* from three different lines were evaluated for FHB resistance using single floret inoculation (*35*). The FHB was scored for at least five spikes per repeat, with at least three repeats for each transgenic line.

resistance to *F. graminearum*, supporting that this gene represents *Fhb7* (fig. S17). Sequence analysis of 22 ethyl methanesulfonate (EMS)–induced mutants identified five amino acids that were implicated in *Fhb7*'s FHB resistance–related function: S34F, T48I, A98V, A9V, and P106L (fig. S18 and data S2). Moreover, two stop-gain mutations at position 209 or 243 led to reduced resistance to *F. graminearum* (fig. S18 and data S2). To confirm Tel7E01T1020600.1 as *Fhb7*, we transgenically introduced a construct with the native promoter and the 846–base pair (bp) coding sequence of this gene into the FHB-disease–susceptible wheat cultivar KN199 and assessed three independent T_3-transgenic plants. The *Fusarium*-inoculated transgenic plants exhibited lower FHB symptom with substantially fewer diseased spikelets per spike than the control (Fig. 1D).

Evolutionary history and molecular function of *Fhb7*

Protein domain–based functional annotation predicted that *Fhb7* likely encodes a GST enzyme. A BLAST search of the *Fhb7* sequence against the National Center for Biotechnology Information (NCBI) GenBank database (*23*) did not find any homolog of *Fhb7* in the *Triticum* genus or in the entire plant kingdom. However, there is a homolog sharing 97% identity in the genome of *E. aotearoae* (Fig. 2A and fig. S19). A phylogenetic analysis of the *Fhb7* sequence revealed its distribution among *Epichloë* species, endophytic fungi of temperate grasses (Fig. 2A). Thus, the occurrence of the *Fhb7* gene in the *Th. elongatum* genome might be caused by fungus-to-plant HGT (FP-HGT) event. Because the *Fhb7* locus is present both in the diploid E genome of *Th. elongatum* and in 7E2 from decaploid *Th. ponticum*, this FP-HGT event apparently occurred after the divergence of the E genome from *Triticum* sp. but before the formation of the decaploid *Th. ponticum* (Fig. 2A).

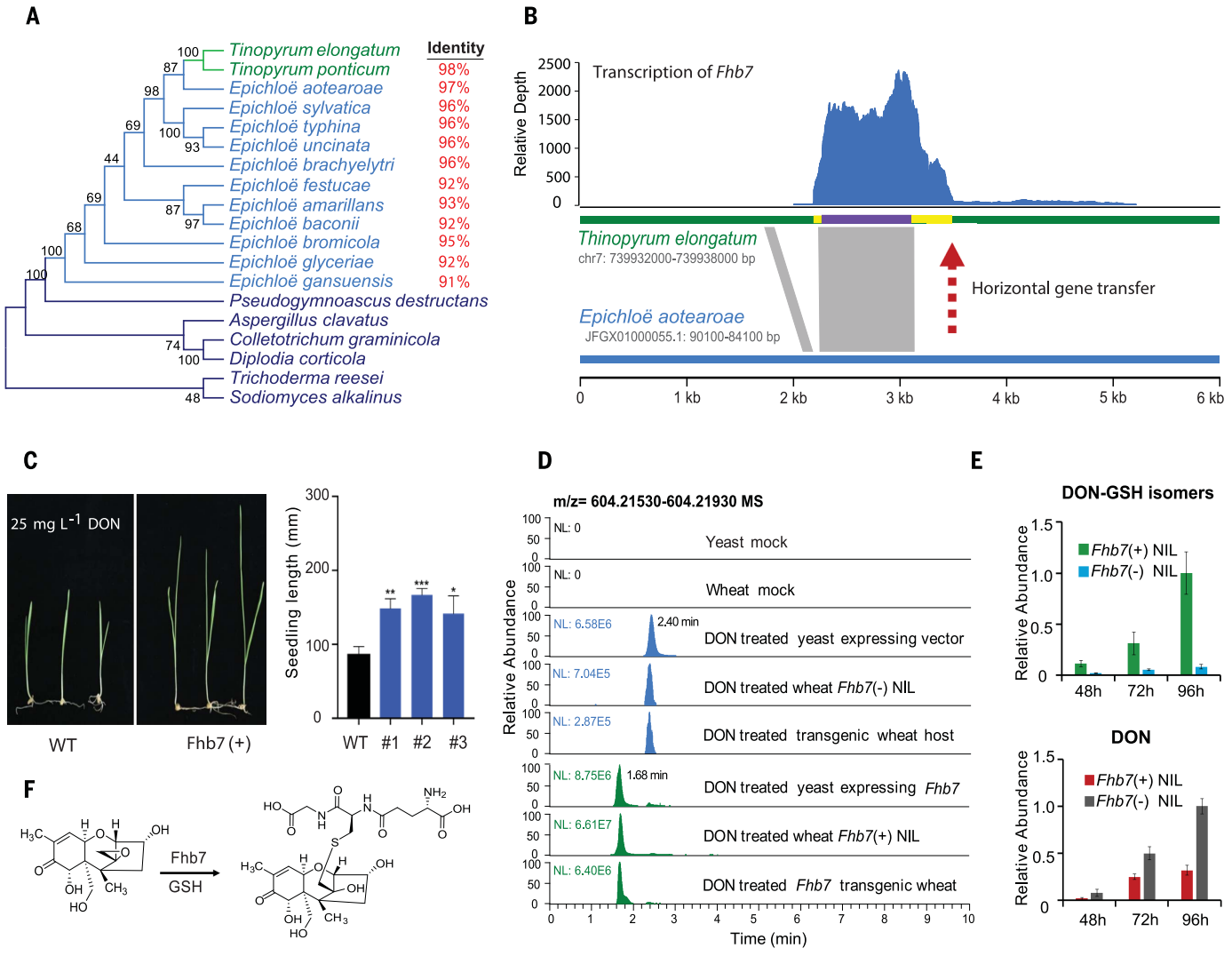

Fig. 2. *Fhb7* confers FHB resistance by detoxifying DON. (**A**) Maximum likelihood phylogenetic tree of the closest homologs of *Fhb7* from plants and fungi. The DNA sequence similarity with *Fhb7* is marked in red. (**B**) Horizontal gene transfer of *Fhb7*. The transcripts CDS (purple), and possible untranslated regions (yellow) of *Fhb7* are shown along chromosome 7E, and the sequence sharing high similarity with the *E. aotearoae* genome is presented as a gray block. The genomic fragment (897 bp) containing full CDS and partial untranslated region of *Fhb7* showed 97% identity between the two genomes. (**C**) DON tolerance of *Fhb7*-transgenic wheat. Seedlings (4 days old) were moved to a petri dish containing 25 mg L^{-1} DON and seedling length was evaluated 7 d after the DON treatment at room temperature. (**D**) Extracted ion chromatograms (EICs) at *m/z* 604.2173 revealing the presence of two DON-glutathione adducts. The *Fhb7* NIL, *Fhb7*-transgenic wheat, and *Fhb7*-transgenic yeast (*P. pastoris*) cultures were treated with 25 mg L^{-1} DON for 24 hours. A product that elutes at 1.68 min accumulated in Fhb7(+) samples and a known, nonenzymatically produced DON-glutathione adduct product that elutes at 2.4 min accumulated in the corresponding *Fhb7*(−) control samples. (**E**) Relative abundances of the de-epoxidated Fhb7-catalyzed DON-glutathione (green) adduct and the known nonenzymatic DON-glutathione adduct (blue) in spikes of *Fusarium*-challenged NIL plants contrasting in *Fhb7*. After inoculation of *F. graminearum* on spike glumes, the *Fhb7*(+) NIL accumulated a copious amount of de-epoxidated DON-glutathione adduct. By contrast, the DON substrate reduced the accumulation in *Fhb7*(+) NIL compared with that in *Fhb7*(−) NIL, as shown in the bottom bar chart. (**F**) Molecular structure of the de-epoxidated DON-glutathione adduct catalyzed by Fhb7.

The horizontal transfer of the *Fhb7* sequence did not occur as a part of a gene cluster (presuming that it is from *E. aotearoae* as the donor genome; this is the species harboring the closest identified homolog of *Fhb7*) (fig. S20). On the basis of sequence similarity, the sequence was transferred into the diploid E genome as a short fragment, including the 846-bp coding sequence for *Fhb7*, a 32-bp sequence before the start codon, and a 19-bp sequence after the stop codon (Fig. 2B). At the position 535 bp upstream of *Fhb7*'s start codon in the E genome, another 90-bp sequence shows high identity to a sequence in *E. aotearoae* (Fig. 2B), suggesting the possibility that a larger sequence was initially transferred to *Th. elongatum* but late mutations occurred in the transferred sequence. The insertion of the *Epichloë* genome fragment in the E genome was also identified in a BAC clone harboring *Fhb7* (Fig. 1C and data S3), confirming that the sequence is not an artifact from the genome assembly process.

Phylogenetic analysis of the GST superfamily showed that *Fhb7* belongs to the fungal GTE (glutathione transferase etherase–related) subfamily (fig. S21 and tables S22 and S23), wherein all members contain a LigE domain, but none of which has been functionally characterized to date (*24*). The *Fhb7* gene is conserved in *Epichloë* species and in multiple *Thinopyrum* species, emphasizing its role in protecting organisms from the cytotoxic damage caused by *Fusarium* species (Fig. 2A and fig. S20).

Gene expression analysis in a time course of *Fusarium* infection in *Th. elongatum* and the 7E2/7D substitution line (table S18) showed that the transcription levels of *Fhb7* were induced at 48 hours after infection (fig. S22).

Research in plant pathology about the progression of *F. graminearum* infection in wheat has established that the fungus starts to produce its DON mycotoxin, an inhibitor of protein synthesis that targets ribosomal machinery, by the 48-hour infection time point (*25*). We therefore conducted DON assays on wheat seedlings of the 7E2/7D substitution line. The results showed that the expression of *Fhb7* can be induced within 6 hours after DON treatment (fig. S22), suggesting that this putative GST enzyme may have a role in xenobiotic detoxification. To test this hypothesis, we conducted a growth inhibition assay by growing *Fhb7* near-isogenic lines (NILs) and *Fhb7*-transgenic wheat seedlings in media containing DON and found that the plants with *Fhb7* grew better (assessed as seedling length) than the plants without *Fhb7* (Fig. 2C and fig. S23). We also expressed *Fhb7* in yeast to test its growth on DON-containing media and found that both the *Fhb7*(+) and *Fhb7*(−) yeasts grew well in the absence of DON; however, only the *Fhb7*(+) yeast grew normally on the media containing 400 mg L^{-1} DON (fig. S24).

Further evidence for the involvement of *Fhb7* in detoxification was demonstrated by its direct use of DON as a substrate. We treated the seedlings of NILs, *Fhb7*-transgenic wheat, and *Fhb7*-expressing yeast cultures with DON, and found that the presence of *Fhb7* in wheat and yeast caused accumulation of a chromatographic peak at 1.68 min, but the accumulation was not detected in the corresponding control samples without *Fhb7* (Fig. 2D). This peak had a mass/charge (m/z) value of 604.2173 (± 3 ppm) under positive ion mode, which is equal to the value for the molecule comprising DON (296.1259), a glutathione group (307.0838), and a hydrogen atom (1.0078), therefore suggesting that *Fhb7* confers GST activity to form a glutathione adduct of DON (DON-GSH) (Fig. 2D and fig. S25).

Previous studies on FHB- and DON-associated chemistry (*26*, *27*) using nuclear magnetic resonance spectroscopy confirmed the nonenzymatic formation of a DON-GSH adduct that was formed through a reaction with the double bond at C10 on DON's first planar ring. This product was mainly detected in the DON-treated *Fhb7*(−) yeast cultures and *Fhb7*(−) wheat samples with the peak at 2.4 min (Fig. 2D and fig. S25). Although the two detected DON-GSH isomers had identical m/z values, tandem mass spectrometry with collision-induced dissociation experiments unequivocally supported that the *Fhb7*(+) samples produce a de-epoxidated DON-GSH adduct (figs. S25 to S28); that is, the GSH group added by Fhb7 is attached to the C13 carbon, which disrupts the epoxy group known to be critical in DON's toxicity (Fig. 2F) (*28*). Further, we used liquid chromatography–high-resolution mass spectrometry (LC-HRMS) to profile DON-treated spikes from 37 diverse wheat germplasm accessions and cultivars without Fhb7. We detected the DON-GSH (C10) peak at 2.4 min in all of these plants but did not detect the 1.68-min de-epoxidated DON-GSH (C13) adduct in any of them (fig. S29).

Fusarium species produce a series of trichothecene mycotoxins, including DON, 3-ADON, 15-ADON, T-2, HT-2, fusarenon-X, NIV, diacetoxyscirpenol, and others, the distribution of which varies among *Fusarium* chemotypes (*24*, *26*). Considering the common occurrence of epoxy groups in these trichothecene compounds, we hypothesized that Fhb7 may be able to detoxify trichothecenes other than DON. Indeed, LC-HRMS analysis of trichothecene-treated wheat samples revealed the presence of GSH adducts for all the trichothecenes that we tested in this study (figs. S30 to S37). In light of Fhb7's wide catalytic spectrum for these mycotoxins, we investigated whether it can confer resistance to other *Fusarium* chemotypes, including *F. pseudograminearum* for crown rot and *F. asiaticum*, a predominant FHB-causing strain in south China. Assays using detached wheat leaves showed that the *Fhb7*-transgenic plants exhibited smaller lesions than wild-type plants for all the tested *Fusarium* species (fig. S38). *F. pseudograminearum* was also inoculated on the base of wheat seedlings, and the results confirmed that the transgenic plants also exhibit improved crown rot resistance compared with the nontransgenic controls (fig. S39). These results further demonstrate how *Th. elongatum* benefits from *Fhb7* through the FP-HGT event, which protects plants from *Fusarium*-caused cytotoxic damage by detoxifying trichothecene through de-epoxidation (fig. S20).

Application of *Fhb7* in *Fusarium* resistance breeding

Considering *Fhb7*'s functionality, specifically in the enzymatic conversion of trichothecenes, we speculated that incorporating the *Fhb7* locus into wheat may confer resistance in different genetic backgrounds without affecting yield traits. Indeed, the translocation of a short fragment [with ~16% of the 7E long arm (*13*)] on wheat 7D resulted in wheat lines with broad resistance to both FHB and crown rot (Fig. 3, A to C). Detailed characterization of NILs (LX99 background) in field conditions showed no significant difference in agronomic yield traits (e.g., thousand grain weight, flag leaf length, etc.; Fig. 3, D and E). Obvious yield penalty caused by *Fhb7* resistance was also not detected when it was transferred into seven additional genetic backgrounds (Fig. 3F and fig. S40). These results demonstrated the advantages of *Fhb7*-mediated resistance over other QTLs, including high resistance to both FHB and crown rot and detoxifying DON without yield penalty, and thus highlighted the potential utility of the *Fhb7* locus in future wheat breeding for improved FHB resistance and good yield traits.

Discussion

Fusarium diseases are economically impactful because of their effects on the production of cereal crops. In this study, the successful cloning of *Fhb7* from the Triticeae E genome and characterization of its molecular mechanism advances the knowledge on the essential role of trichothecenes in the pathogenesis of *Fusarium*. We have demonstrated that *Fhb7* confers FHB resistance in diverse wheat genetic backgrounds without yield penalty and Fhb7 is able to biochemically detoxify trichothecene mycotoxins produced by multiple *Fusarium* species, which highlights the value of *Fhb7* in combating FHB and reducing DON contamination in wheat and other cereal crops through breeding.

The epoxides at the C12/13 of trichothecene mycotoxins are the key contributors to their toxicity. However, to date, genes or proteins with de-epoxidation function have not been identified (*3*). *Fusarium* species can reduce DON toxicity by adding an acetyl group on the hydroxyl group at C3 and C15, forming 3-ADON and 15-ADON, respectively; however, the reduction of cytotoxicity for these DON derivatives is modest in plant cells (*3*). In planta, glucosylation at C3 has been documented to detoxify DON by forming DON-3-glucoside (D3G), which is reversible in animals, causing release of DON during digestion (*29*). Here, beyond our identification of an FHB resistance gene, the broad detoxification spectrum of Fhb7 through de-epoxidation of trichothecenes suggests the potential utility of the GST enzyme in the biomedicine, feed, and food industries in addition to reducing DON content in wheat grain.

HGT, the transfer of genes between nonmating species, is thought to occur frequently in prokaryotes, but much less so in eukaryotes (*30*). There is accumulating evidence illustrating instances of HGT events involving bacteria or the organellar genomes of another plant as donor (*31*). For instance, two *Agrobacterium* genes were found to be inserted in the genome (with transfer DNA borders) of a cultivated sweet potato [*Ipomoea batatas* (L.) Lam.], revealing a naturally occurring transgenic food crop (*32*). However, there is little evidence for HGT events involving nuclear DNA transmission from fungi or other eukaryotes, and such transmission has been thought to be insignificant (*33*). Fundamentally, our results highlight the roles that FP-HGT has had in shaping plant genomes, which advances the

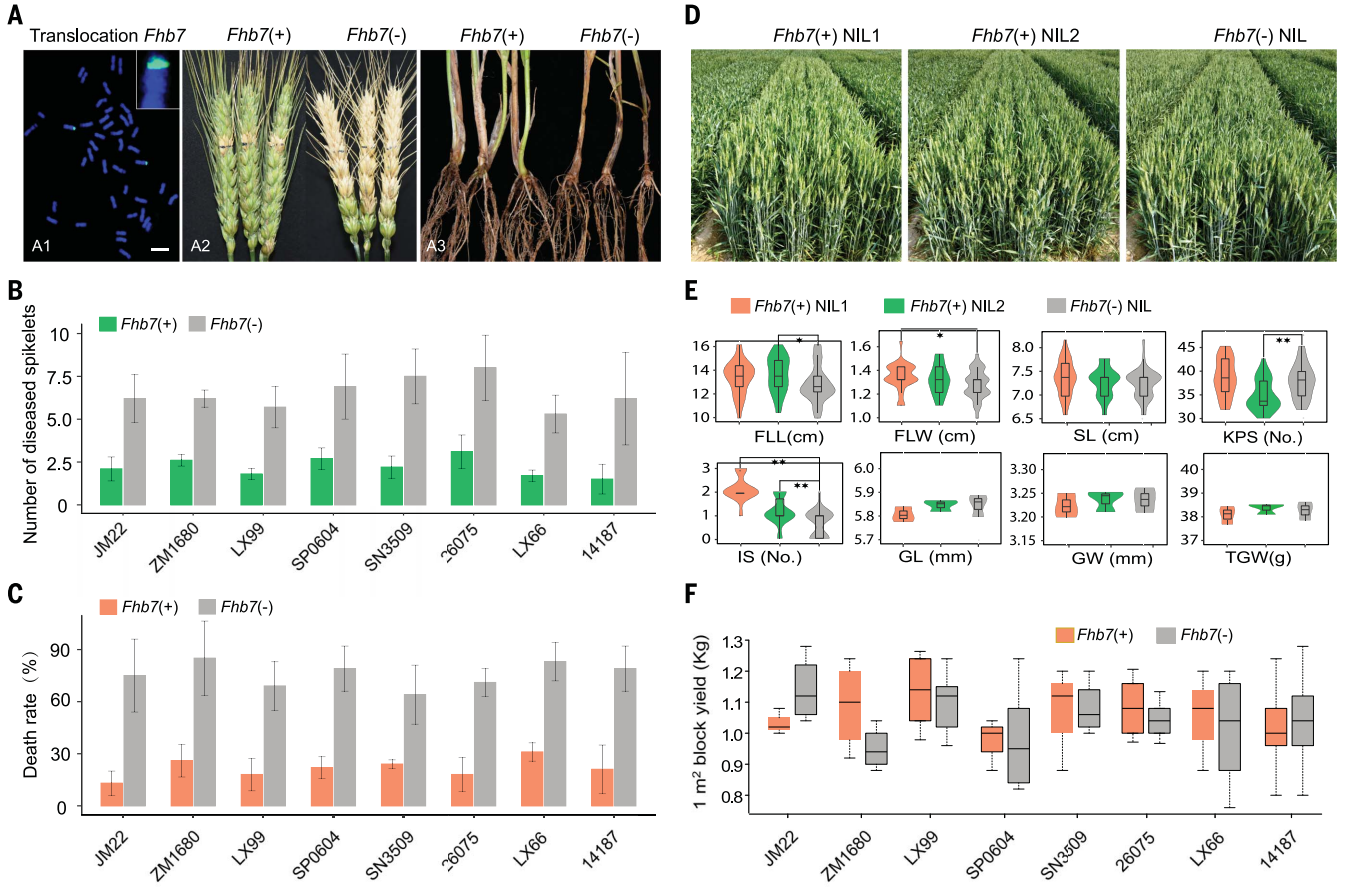

Fig. 3. Application prospects for *Fhb7* in wheat resistance breeding. (**A**) Genomic in situ hybridization analysis (left panel) showing a translocation of the distal region of 7E (containing *Fhb7*) from an E genome donor into wheat. Scale bar, 20 μm. Also shown are images of *Fusarium*-infected spikes (middle panel) and crown rot (right panel) of LX99 NILs contrasting in *Fhb7*. (**B**) FHB resistance of *Fhb7* in eight different wheat genetic backgrounds evaluated at 21 d after inoculation in field conditions. (**C**) Crown rot phenotypes were recorded as the death ratio after growth in soil containing *F. pseudograminearum* at 30 days postinfection. (**D**) Field plant photographs of two *Fhb7*(+) NILs and one *Fhb7*(−) NIL in the LX99 background. (**E**) Comparison of the yield traits among the two *Fhb7*(+) NILs and one *Fhb7*(−) NIL in the LX99 background evaluated in the 2017 field experiment. FLL, flag leaf length (cm); FLW, flag leaf width (cm); SL, spike length (cm); KPS, kernels per spike; IS, infertile spikelets; GL, grain length (mm); GW, grain width (mm); TGW, thousand grain weight (g). (**F**) Comparison of the grain yield among eight *Fhb7* translocation lines in different wheat genetic backgrounds. The grain yield was measured from a 1-m^2 plot in the 2017 and 2018 field experiments.

knowledge on disease resistance gene evolution and opens a new avenue for the identification of plant resistance genes.

The endophytic *Neotyphodium* and *Epichloë* fungi often form mutualistic symbiotic associations with forage grasses and offer hosts bioprotective benefits against pathogens and abiotic stresses, presumably owing to the fungus-mediated anabolism and catabolism of various natural product compounds (*34*). Here, we showed that the GST encoded by *Fhb7* is conserved in *Epichloë* species and is able to detoxify the trichothecene mycotoxins secreted by *Fusarium* species. Thus, transfer of this fungal gene into a plant genome could be beneficial to plants, perhaps even eliminating the need for the symbiotic association per se. The finding of *Fhb7*-mediated resistance to both FHB and crown rot diseases further emphasizes the importance of this HGT in benefiting the perennial *Th. elongatum*, which is perhaps reflected by constitutive expression of *Fhb7* in all examined tissues. However, the molecular machinery that enabled the FP-HGT of *Fhb7* and the nature of the promoter evolution underlying the expression of *Fhb7* remain to be elucidated.

Methods summary

The *Th. elongatum* genome was first sequenced by Illumina short-read sequencing and was de novo assembled using the software package DeNovoMAGICTM3.0. PacBio SMRT long reads were used to fill the gaps in the assembly and Bionano optical maps were then used to correct and extend the scaffold sequences. The assembly was anchored into seven pseudochromosomes using Hi-C data. The assembly was validated using independent BAC sequences, genetic maps of related species, and commonly used software programs. Genes, repetitive DNA, and other genomic features in the assembly were annotated to reveal the landscape of the species and to examine their relationship with wheat and other related species by in-depth comparative analyses. Genetic markers in the *Fhb7* region were developed by means of the reference genome sequence and used to screen recombinants for fine mapping to identify the *Fhb7* candidate gene. The candidate gene was functionally validated by virus-induced gene silencing, EMS-induced mutation, and transgenic approaches. FHB resistance was evaluated by inoculation of *Fusarium* conidial suspensions on wheat spikes, leaves, or crowns. LC-HRMS(/MS) analysis was used to infer the biochemical structure of trichothecene-glutathione adducts catalyzed by Fhb7. *Fhb7* was introgressed into diverse wheat backgrounds using distant hybridization and conventional breeding, and the presence of alien chromatin in wheat was validated by genomic in situ hybridization.

REFERENCES AND NOTES

1. J. K. Haile *et al*., *Fusarium* head blight in durum wheat: Recent status, breeding directions, and future research prospects. *Phytopathology* **109**, 1664–1675 (2019). doi: 10.1094/PHYTO-03-19-0095-RVW; pmid: 31369363
2. F. Trail, For blighted waves of grain: *Fusarium graminearum* in the postgenomics era. *Plant Physiol.* **149**, 103–110 (2009). doi: 10.1104/pp.108.129684; pmid: 19126701
3. A. Hathout, S. Aly, Biological detoxification of mycotoxins: A review. *Ann. Microbiol.* **64**, 905–919 (2014). doi: 10.1007/s13213-014-0899-7
4. Y. Hao, A. Rasheed, Z. Zhu, B. B. H. Wulff, Z. He, Harnessing wheat *Fhb1* for *Fusarium* resistance. *Trends Plant Sci.* **25**, 1–3 (2020). doi: 10.1016/j.tplants.2019.10.006; pmid: 31679993
5. E. S. Lagudah, S. G. Krattinger, A new player contributing to durable *Fusarium* resistance. *Nat. Genet.* **51**, 1070–1071 (2019). doi: 10.1038/s41588-019-0454-3; pmid: 31253973
6. G. Li *et al*., Mutation of a histidine-rich calcium-binding-protein gene in wheat confers resistance to *Fusarium* head blight. *Nat. Genet.* **51**, 1106–1112 (2019). doi: 10.1038/s41588-019-0426-7; pmid: 31182810
7. Z. Su *et al*., A deletion mutation in *TaHRC* confers *Fhb1* resistance to *Fusarium* head blight in wheat. *Nat. Genet.* **51**, 1099–1105 (2019). doi: 10.1038/s41588-019-0425-8; pmid: 31182809
8. N. Rawat *et al*., Wheat *Fhb1* encodes a chimeric lectin with agglutinin domains and a pore-forming toxin-like domain conferring resistance to *Fusarium* head blight. *Nat. Genet.* **48**, 1576–1580 (2016). doi: 10.1038/ng.3706; pmid: 27776114
9. L. Cui *et al*., Development of perennial wheat through hybridization between wheat and wheatgrasses: A review. *Engineering* **4**, 507–513 (2018). doi: 10.1016/j.eng.2018.07.003
10. X. Zhang *et al*., A genetic map of *Lophopyrum ponticum* chromosome 7E, harboring resistance genes to *Fusarium* head blight and leaf rust. *Theor. Appl. Genet.* **122**, 263–270 (2011). doi: 10.1007/s00122-010-1441-3; pmid: 20830464
11. L. L. Qi, M. O. Pumphrey, B. Friebe, P. D. Chen, B. S. Gill, Molecular cytogenetic characterization of alien introgressions with gene *Fhb3* for resistance to *Fusarium* head blight disease of wheat. *Theor. Appl. Genet.* **117**, 1155–1166 (2008). doi: 10.1007/s00122-008-0853-9; pmid: 18712343
12. C. Ceoloni *et al*., Cytogenetic mapping of a major locus for resistance to *Fusarium* head blight and crown rot of wheat on *Thinopyrum elongatum* 7EL and its pyramiding with valuable genes from a *Th. ponticum* homoeologous arm onto bread wheat 7DL. *Theor. Appl. Genet.* **130**, 2005–2024 (2017). doi: 10.1007/s00122-017-2939-8; pmid: 28656363
13. J. Guo *et al*., High-density mapping of the major FHB resistance gene *Fhb7* derived from *Thinopyrum ponticum* and its pyramiding with *Fhb1* by marker-assisted selection. *Theor. Appl. Genet.* **128**, 2301–2316 (2015). doi: 10.1007/s00122-015-2586-x; pmid: 26220223
14. H. Li, X. Wang, *Thinopyrum ponticum* and *Th. intermedium*: The promising source of resistance to fungal and viral diseases of wheat. *J. Genet. Genomics* **36**, 557–565 (2009). doi: 10.1016/S1673-8527(08)60147-2; pmid: 19782957
15. X. Shen, H. Ohm, Molecular mapping of *Thinopyrum*-derived *Fusarium* head blight resistance in common wheat. *Mol. Breed.* **20**, 131–140 (2007). doi: 10.1007/s11032-007-9079-9
16. R. P. Singh, R. A. McIntosh, Genetics of resistance to *Puccinia graminis* tritici in 'Chris' and 'W3746' wheats. *Theor. Appl. Genet.* **73**, 846–855 (1987). doi: 10.1007/BF00289389; pmid: 24241294
17. R. M. Waterhouse *et al*., BUSCO Applications from quality assessments to gene prediction and phylogenomics. *Mol. Biol. Evol.* **35**, 543–548 (2018). doi: 10.1093/molbev/msx319; pmid: 29220515
18. S. Ou, J. Chen, N. Jiang, Assessing genome assembly quality using the LTR Assembly Index (LAI). *Nucleic Acids Res.* **46**, e126 (2018). doi: 10.1093/nar/gky730; pmid: 30107434
19. T. Kantarski *et al*., Development of the first consensus genetic map of intermediate wheatgrass (*Thinopyrum intermedium*) using genotyping-by-sequencing. *Theor. Appl. Genet.* **130**, 137–150 (2017). doi: 10.1007/s00122-016-2799-7; pmid: 27738715
20. B. S. Gaut, B. R. Morton, B. C. McCaig, M. T. Clegg, Substitution rate comparisons between grasses and palms: Synonymous rate differences at the nuclear gene Adh parallel rate differences at the plastid gene rbcL. *Proc. Natl. Acad. Sci. U.S.A.* **93**, 10274–10279 (1996). doi: 10.1073/pnas.93.19.10274; pmid: 8816790
21. J. Guo *et al*., Molecular and cytological comparisons of chromosomes $7el_1$, $7el_2$, $7E^e$, and $7E^t$ derived from *Thinopyrum*. *Cytogenet. Genome Res.* **145**, 68–74 (2015). doi: 10.1159/000381838; pmid: 25968454
22. X. Shen, L. Kong, H. Ohm, *Fusarium* head blight resistance in hexaploid wheat (*Triticum aestivum*)-*Lophopyrum* genetic lines and tagging of the alien chromatin by PCR markers. *Theor. Appl. Genet.* **108**, 808–813 (2004). doi: 10.1007/s00122-003-1492-9; pmid: 14628111
23. S. F. Altschul, W. Gish, W. Miller, E. W. Myers, D. J. Lipman, Basic local alignment search tool. *J. Mol. Biol.* **215**, 403–410 (1990). doi: 10.1016/S0022-2836(05)80360-2; pmid: 2231712
24. M. Morel, A. A. Ngadin, M. Droux, J. P. Jacquot, E. Gelhaye, The fungal glutathione S-transferase system. Evidence of new classes in the wood-degrading basidiomycete *Phanerochaete chrysosporium*. *Cell. Mol. Life Sci.* **66**, 3711–3725 (2009). doi: 10.1007/s00018-009-0104-5; pmid: 19662500
25. S. Walter, P. Nicholson, F. M. Doohan, Action and reaction of host and pathogen during *Fusarium* head blight disease. *New Phytol.* **185**, 54–66 (2010). doi: 10.1111/j.1469-8137.2009.03041.x; pmid: 19807873
26. B. Kluger *et al*., Stable isotopic labelling-assisted untargeted metabolic profiling reveals novel conjugates of the mycotoxin deoxynivalenol in wheat. *Anal. Bioanal. Chem.* **405**, 5031–5036 (2013). doi: 10.1007/s00216-012-6483-8; pmid: 23086087
27. S. A. Gardiner *et al*., Transcriptome analysis of the barley-deoxynivalenol interaction: Evidence for a role of glutathione in deoxynivalenol detoxification. *Mol. Plant Microbe Interact.* **23**, 962–976 (2010). doi: 10.1094/MPMI-23-7-0962; pmid: 20521958
28. A. Stanic *et al*., Characterization of deoxynivalenol–glutathione conjugates using nuclear magnetic resonance spectroscopy and liquid chromatography–high-resolution mass spectrometry. *J. Agric. Food Chem.* **64**, 6903–6910 (2016). doi: 10.1021/acs.jafc.6b02853; pmid: 27548277
29. F. Berthiller *et al*., Occurrence of deoxynivalenol and its 3-β-D-glucoside in wheat and maize. *Food Addit. Contam. Part A Chem. Anal. Control Expo. Risk Assess.* **26**, 507–511 (2009). doi: 10.1080/02652030802555668; pmid: 19680925
30. F. Husnik, J. P. McCutcheon, Functional horizontal gene transfer from bacteria to eukaryotes. *Nat. Rev. Microbiol.* **16**, 67–79 (2018). doi: 10.1038/nrmicro.2017.137; pmid: 29176581
31. P. J. Keeling, J. D. Palmer, Horizontal gene transfer in eukaryotic evolution. *Nat. Rev. Genet.* **9**, 605–618 (2008). doi: 10.1038/nrg2386; pmid: 18591983
32. T. Kyndt *et al*., The genome of cultivated sweet potato contains *Agrobacterium* T-DNAs with expressed genes: An example of a naturally transgenic food crop. *Proc. Natl. Acad. Sci. U.S.A.* **112**, 5844–5849 (2015). doi: 10.1073/pnas.1419685112; pmid: 25902487
33. H. Shinozuka *et al*., Horizontal transfer of a ß-1,6-glucanase gene from an ancestral species of fungal endophyte to a cool-season grass host. *Sci. Rep.* **7**, 9024 (2017). doi: 10.1038/s41598-017-07886-2; pmid: 28831055
34. A. Tanaka, D. Takemoto, T. Chujo, B. Scott, Fungal endophytes of grasses. *Curr. Opin. Plant Biol.* **15**, 462–468 (2012). doi: 10.1016/j.pbi.2012.03.007; pmid: 22465162
35. L. Zhao *et al*., Cloning and characterization of a specific UDP-glycosyltransferase gene induced by DON and *Fusarium graminearum*. *Plant Cell Rep.* **37**, 641–652 (2018). doi: 10.1007/s00299-018-2257-x; pmid: 29372381

ACKNOWLEDGMENTS

We thank Q. Song (Lanzhou University) and X. Zhang (University of Louisville) for advice on entophytic fungi and biochemical analysis of trichothecenes, X. L. Zhang (Northeast Forestry University) for providing some marker sequences of the Triticeae E genome, and Y. Liang and J. Yu (Shandong Agricultural University) for providing the *Fusarium* stains. **Funding**: This work was supported by the National Natural Science Foundation of China (31520103911, 31871610, and 31901492), the National Key Research and Development Program (2016YFD0100102-2), the National Key Program on Transgenic Research from the Ministry of Agriculture of China (2016ZX08002003-002 and 2016ZX08009-003), and the Agricultural Variety Improvement Project of Shandong Province (2019LZGC016). **Author contributions**: H.W. and L.K. designed the project. S.S.X., G.B., E.N., C.G., and H.O. supervised the project. S.S., K.W., L.C., X.F., and F.N. performed bioinformatics analysis. W.G., L.Z., B.H., Z.L., S.S.X., J.G., M.L., P.S., X.F.L., G.W., C.B., W.Z., X.C., J.W., L.D., W.C., W.L., G.X., J.Z., Y.H., Y.X., Y.G., W.J.L., Y.L., H.Y., J.L., X.L., Y.Z., and X.W. conducted experiments. X.M. and A.L. performed the field work. H.W., S.S., G.B., and L.K. wrote the paper with input from all authors. **Competing interests:** The authors declare no competing interests. Patents with application nos. 202010146400 9 and 202010146399X are pending. **Data and materials availability:** All data are available in the manuscript, the supplementary materials, or at publicly accessible repositories. These data in the public repositories include all raw reads and assembled sequence data for *Th. elongatum* in NCBI under BioProjectID PRJNA540081, the assembly and annotation data of *Th. elongatum*, and the draft genomes of 7E/7D substitution lines in the Genome Warehouse in BIG Data Center under accession numbers GWHABKY00000000, GWHABLF00000000, and GWHABLE00000000, which are accessible at https://bigd.big.ac.cn/gwh. All materials are available from L. Kong upon request.

SUPPLEMENTARY MATERIALS

science.sciencemag.org/content/368/6493/eaba5435/suppl/DC1
Materials and Methods
Figs. S1 to S40
Tables S1 to S23
Captions for Data S1 to S3
References (*36*–*93*)
MDAR Reproducibility Checklist
Data S1 to S3

View/request a protocol for this paper from *Bio-protocol*.

12 December 2019; accepted 26 March 2020
Published online 9 April 2020
10.1126/science.aba5435